Internal and surface temperature profiles of spherical biosolids particles during convective drying

Julian Nylen, Madoc Sheehan, Anna Whelan & Elsa Antunes

View supplementary material ☑

Published online: 26 Sep 2024.

Submit your article to this journal ☑

Article views: 94

View related articles ☑

View Crossmark data ☑

Taylor & Francis
Taylor & Francis Group

Internal and surface temperature profiles of spherical biosolids particles during convective drying

Julian Nylen[a] , Madoc Sheehan[a], Anna Whelan[b], and Elsa Antunes[a]

[a]College of Science & Engineering, James Cook University, Townsville, Australia; [b]Townsville City Council, Townsville, Australia

ABSTRACT

The convective drying of spherical biosolids particles from two wastewater treatment plants (Type 1: anaerobic/anoxic treatment with belt filter press dewatering; Type 2: aerobic/anoxic treatment with centrifuge dewatering) was studied under 10 conditions across 44 trials. A wide spectrum of conditions including three drying temperatures (88, 109, and 138 °C), two gas velocities (1.6 and 2 m s^{-1}), and particle sizes of 2 cm and 4 cm were investigated. Measured variables included particle mass, center/internal temperature, surface temperature, shrinkage, and qualitative observations of morphological changes. Most samples showed two drying periods, a constant rate period followed by a falling rate period. Additionally, it was found that drying rates and morphological changes depended significantly on particle size and drying intensity (i.e., drying gas temperature and gas velocity) with higher intensities resulting in larger, more porous particles. Internal temperature profiles displayed a consistent pattern, an initial heating phase where internal temperatures quickly rose to approximately the wet bulb temperature of the drying gas, a quasi-constant temperature phase at that temperature, and a final sharp increase/spike to reach equilibrium with the drying gas temperature. Moreover, IR images showed that sub-surface temperatures (between the core and surface) were significantly lower than surface temperatures. Surface temperatures showed a more linear increase throughout drying until equilibrium with the drying gas temperature. The consistent temperature difference between the center and surface, as well as the internal temperature profile, suggests the existence of a drying front, moving radially inward as the particle dries. This research contributes to a better understanding of biosolids drying dynamics, offering insights to improve thermal treatment strategies thereby contributing to the broader field of waste management.
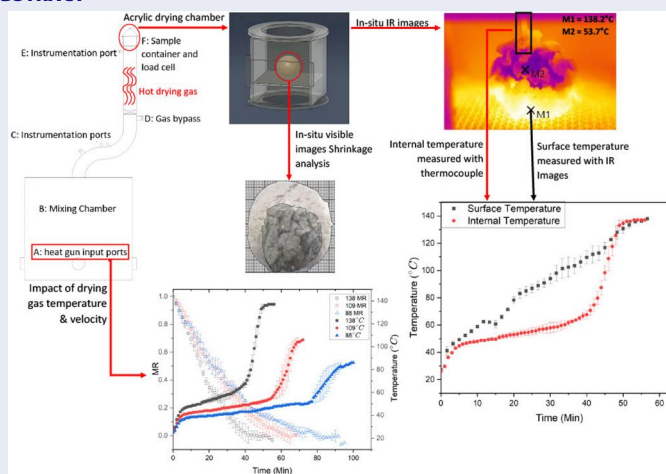
GRAPHICAL ABSTRACT

1. Introduction

Biosolids are a complex heterogeneous mixture of organic matter (50%–70% of dry mass), nutrients, and water (typically 80% on a wet basis) and are generated as a by-product of wastewater treatment plant (WWTP) processes.[1] Historically considered a waste, advancements in wastewater treatment technologies coupled with an emphasis on environmental sustainability and an adoption of circular economy principles, have repositioned biosolids as a valuable resource. Rich in organic matter and nutrients, such as nitrogen and phosphorus, which are critical for soil health and plant growth, biosolids have gained significant attention for their role in sustainable land application practices, such as agriculture, forestry, and land reclamation.[2,3] This use captures biosolids fertilizing and soil amendment properties, providing an environmentally friendly and economically viable alternative to traditional disposal methods, such as carbon emission-intensive incineration and costly landfilling.[3]

Despite their benefits, the application of biosolids is not without its challenges. The production of biosolids in Australia was approximately 380,000 tons of dry solids in 2021, illustrating the scale of biosolids generated annually.[4] Furthermore, as production is inherently linked to population growth, this volume is expected to increase as populations continue to rise. A significant concern in the management of biosolids is the presence of contaminants of emerging concern (CECs). These compounds, which are a range of pollutants, include both newly identified and existing chemicals which have adverse environmental and health impacts, have raised questions regarding the safety and sustainability of biosolids application.[5–7] Traditional WWTPs often fail to effectively mitigate these contaminants,[8,9] leaving them in the final biosolids and leading to their potential bioaccumulation.[2,3,5,10–15] This issue is further compounded by tightening regulatory requirements concerning CEC concentrations in biosolids and soils, which poses a significant hurdle to their beneficial reuse.[16]

In response to the challenges posed by CECs thermal treatment methods, such as pyrolysis and gasification, have been identified as promising approaches for biosolids management. These technologies not only promise to destroy/remove CECs through thermolysis, but also convert biosolids into biochar, a carbon-rich material that retains many of the beneficial properties of biosolids while offering the additional environmental benefit of carbon sequestration.[1,17] However, the feasibility of these thermal treatment processes is critically dependent on the substantial reduction of moisture content in biosolids, with economic viability requiring a moisture content below 15%.[18] Given that tertiary sludge has a moisture content of 97-99%,[19] this is a challenging task. Many WWTPs employ mechanical dewatering, which can achieve moisture contents of 80% by removing 'free water', however this is far from the required 15%. The remaining 'bound' water requires thermal drying which requires substantial energy. For example, drying biosolids from a 90% to a 10% moisture content requires approximately $2.5–3 \times 10^6$ kJ/(ton of biosolids) of energy.[20] This highlights the importance of optimizing drying processes to avoid the thermal treatment of biosolids from becoming uneconomical and a financial burden for WWTP owners.

CECs destruction/mineralization hinges off the ability of the system to maintain the contaminants at thermolysis temperatures within the reactor before they volatize and exit.[21] Fundamentally, these systems are primarily designed for effective heat transfer. Particles can be classified as isothermal (lumped) or non-isothermal during thermal treatments (i.e., whether the particles temperature is constant throughout or if there is a temperature gradient). Two major factors that determine this behavior are particle size and moisture content. Larger particles are more likely to experience temperature gradients, while moisture within the particle can act as a heat sink.[22] However, small amounts of moisture within the particle may be beneficial as moisture may also help expedite the thermolysis of some CECs.[23] Hence, it is essential to understand the intricate dynamics of biosolids drying and the role of biosolids properties, such as moisture content and particle size, and what impact these may have on thermal treatment processes.

While many studies have researched biosolids drying, few studies have investigated the internal conditions during the drying process, such as temperature and moisture distributions. Additionally, most research has focused on flat biosolid layers[24–26] with few studies investigating the drying behavior of individual biosolid particles. One of the few papers that investigated internal temperature distribution during drying was by Font et al.,[27] which used biosolids spheres and cylinders (2.5–3 cm) from two different WWTPs. Internal temperature measurements were made by inserting a thin thermocouple into the spheres. Samples were convectively dried at low temperatures between 32 °C and 64 °C with varying gas velocities between 2.4 and 5.5 m/s. Their results revealed that central temperature measurements exhibited a phase of quasi-constant temperature

before undergoing a rapid spike. Furthermore, when a particle was split partway through drying, it revealed three distinct layers: a wet inner core, an intermediate section, and a dry external crust/skin. Both samples exhibited complex morphological changes, such as, shrinkage, skin layer formation, and cracking. Interestingly one sample formed a much more pronounced skin layer than the other, indicating that depending on biosolids composition, drying behavior may differ.[28]

Varying behavior has also been observed by Leonard et al.,[29] who convectively dried two different biosolids, one which had a nutrient removal stage, whilst the other was left untreated. Temperatures ranged from 120 °C to 140 °C, with gas velocities between 1.58 and 1.82 m/s. External mass transfer appeared to be the rate limiting process of the high nutrient biosolids, as indicated by the long constant drying period. Contrastingly, the low nutrient biosolids, which always dried slower, exhibited a long decreasing (falling) drying rate from the onset of drying, indicating diffusion limitations.

Fraikin et al.[30] performed convective drying of cylindrical biosolids samples, measuring 15 mm × 15 mm and weighing approximately 3.5 g, sourced from three different WWTPs.[30] The drying conditions used were: drying gas temperatures of 80 °C, 90 °C, 140 °C, and 200 °C; air velocities between 1 and 3 m/s; and varying absolute humidities of 0.005, 0.084, 0.05, and 0.2 $\frac{Kg_w}{Kg_{da}}$. Key parameters measured included the mass, surface temperature (monitored via a pyrometer), and visual observations. Analysis of the mass versus time data revealed an initial adjustment phase with minimal mass loss, which then transitioned into a prolonged falling rate phase. Surface temperatures exhibited a consistent trend: an initial rapid rise, followed by a period of relative stability, and a final rapid spike in temperature until equilibrium with the drying gas. Results showed that maximum flux was achieved with increased velocity and temperature of the drying gas, coupled with decreased drying gas humidity. Additionally, complex rheological behavior, such as the formation of a hard crust/skin layer, was observed to reduce the drying flux.

The objective of this research is to improve our understanding of the convective drying of biosolids, by experimentally measuring both internal and surface temperatures simultaneously during drying. To the authors' best knowledge, simultaneous internal and surface temperature measurements have not been previously performed for the convective drying of biosolids.

2. Methodology

2.1. Materials

Biosolids were sourced locally from two WWTPs in Townsville, QLD, Australia: the Mt St John (MSJ) plant and the Cleveland Bay (CB) plant. The treatment process at the MSJ plant includes various anoxic and aerobic stages, finishing with an aerobic digester and dewatering via belt filter presses. Conversely, the CB plant uses an anaerobic/anoxic treatment approach, with dewatering achieved via centrifuge. Approximately 5 kg of biosolids were collected from each plant, vacuum-sealed, and refrigerated at 4 °C. From these bulk samples, three sets of 100 g were used for proximate and ultimate analyses, the results of which are shown in Table 1. The remaining bulk samples were used for the drying experiments.

Samples were shaped into 2 cm and 4 cm diameter spheres using 3D printed molds (Figure A1, see Supplementary appendix), consisting of two hemispheres. To closely match the consistency and density of the original sample, only mild compression was used during the shaping process. The 2 cm and 4 cm samples weighed approximately 4.2 g and 34.5 g, respectively.

2.2. Dryer apparatus

A convective drying apparatus (Figure 1(A)) capable of in-situ mass measurements and controlled gas conditions was used to characterize biosolids drying. This apparatus has been successfully used to characterize sugarcane bagasse[31] and algae drying.[32] By adjusting the settings on the four heat guns, the drying gas temperature and gas velocity were controlled. A K-type thermocouple was used to determine the drying gas temperature, while a pitot tube and manometer were used to determine gas velocity. Experiments were conducted in a large air-conditioned room with constant environmental conditions of 23 °C and relative humidity of 50%.

In-situ mass was measured using an OMEGA LCAE-1kg load cell (OMEGA Engineering, CT, USA) in conjunction with a data logger. The logger recorded data at 5-s intervals. To mitigate the impact of gas drag on the accuracy of the mass measurements, a gas bypass was engaged every 3 min for 15 s, and mass data were averaged over this sampling period. Internal/center temperature measurements were collected by inserting a small k-type thermocouple into the biosolids particle, with temperatures being recorded at 1-min intervals. A depth probe was used to help accurately place the thermocouple.

Table 1. Ultimate and proximate analysis of MSJ and CB biosolids samples.

	MSJ	CB
Sludge treatment	Aerobic/Anoxic finalizing with aerobic digester	Anaerobic/Anoxic
Dewatering method	Belt filter press	Centrifuge
Proximate analysis		
Moisture Content	87.0	83.1
Ash	28.5	26.4
Volatile Matter	51.3	54.2
Fixed Carbon	10.4	20.7
Ultimate analysis		
Carbon	31.0	38.3
Total Hydrogen	5.4	5.7
Nitrogen	5.3	6.8
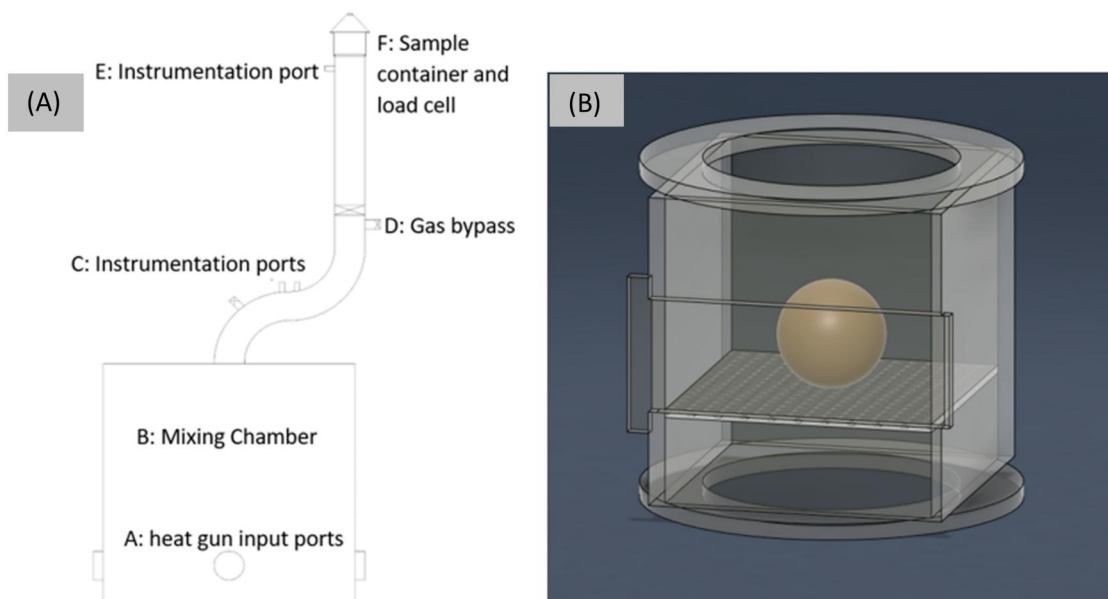
Figure 1. (A) Convective drying apparatus;[27,28] (B) Rendering of Acrylic drying chamber with biosolids particle.

The drying chamber was made from acrylic (Figure 1(B)) to allow for in-situ visual image collection *via* a GoPro Hero 5 Black camera, with images captured every minute. ImageJ was used for image processing to determine particle size and shrinkage. For IR images to be captured unobstructed, a sliding window was built into the chamber and only opened briefly for IR image capture using a TESTO 885. IR images were captured approximately every 2–3 min and processed using 'IRSoft'.

2.3. Experimental design

Temperatures investigated were 88 °C, 109 °C, and 138 °C representing values below, approximately at, and above water's boiling point, respectively. Moreover, as the energy requirements for drying biosolids is substantial, secondary heat sources should be used to increase energy efficiency, with secondary heat sources generally having relatively low temperatures.[33–35] The chosen particle sizes reflected the range observed at the Logan City Council pilot scale gasification plant,[36] with an emphasis

placed on larger particles due to their extended drying time and likely variations in internal temperature and moisture distributions. Gas velocities of 2.4 and 1.6 m/s were investigated, which fall within the range used in other studies,[27,29,30,37] and are typical for industrial convective drying equipment. Table 2 shows the experimental designs, conditions, and the number of trials/repeats for each run/condition. It should be noted that the mass and internal temperature measurements were taken during separate experiments, as the thermocouple influenced the mass measurement of the particle by supporting material, particularly as it shrunk and deformed. Standard deviations for both temperature and MR measurements were calculated using Excel's STDEV.P function, applied to the respective trials for each data point.

3. Results and discussion

Table 1 presents the ultimate and proximate analysis of the MSJ and CB samples. The proximate analysis showed that MSJ, which is dewatered using belt filter presses, had a slightly higher moisture content than the centrifuged

Table 2. Experimental conditions and repetitions for drying experiments.

Run	Internal Temperature Trials	Surface Temperature Trials	Mass Trials	Sample Origin	Diameter (cm)	Drying Gas Temperature (°C)	Gas Velocity (m s⁻¹)
	3	2	3	MSJ	2	138	2.4
2	3	2	3	MSJ	2	109	2.4
3	2	2	2	MSJ	2	88	2.4
4	1	1	2	MSJ	2	138	1.6
5	1	1	1	MSJ	4	138	1.6
6	2	2	2	MSJ	4	138	2.4
7	3	2	3	CB	2	138	2.4
8	3	2	3	CB	2	109	2.4
9	2	2	2	CB	2	88	2.4
10	2	2	1	CB	4	138	2.4

MSJ: Mount St John (predominantly aerobic process); CB: Cleveland Bay (predominately anaerobic process).
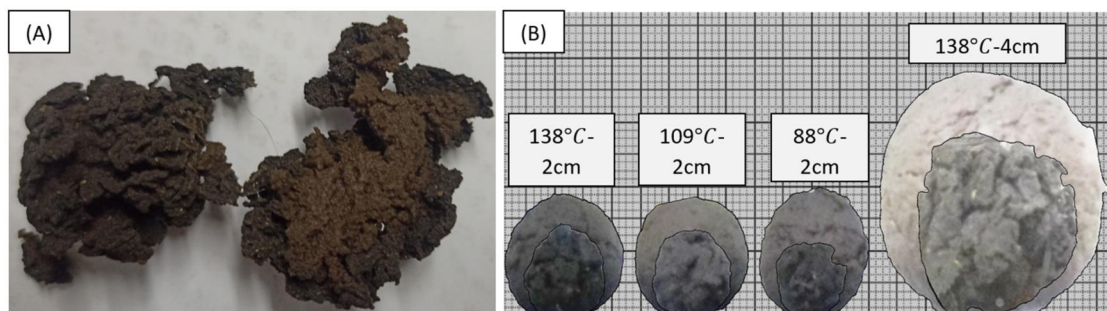

Figure 2. (A) Bisected biosolids particle midway through drying showing a clear distinction between wet core and dry outer crust; (B) Particles pre and post drying, showcasing shrinkage. All particles are from MSJ and had a drying gas velocity of 2.4 m s⁻¹. Titles above particles indicate drying gas temperature and initial particle diameter.

Cleveland Bay samples. Additionally, the ash content of the MSJ samples is slightly higher, while the fixed carbon of MSJ is significantly lower. The ultimate analysis showed that CB samples contain higher levels of carbon and nitrogen than MSJ, indicating potential differences in composition and energy content of the biosolids.

3.1. Morphological changes for various drying intensities

Throughout all runs it was observed that both MSJ and CB particles developed a brittle, dark-colored, porous dry crust. Figure 2(A) shows a 4 cm biosolids particle bisected midway through drying, revealing a distinct moist core and a dry porous outer layer. While direct porosity measurements were not conducted, estimates were made by comparing the material's real density (determined *via* Archimedes' principle/volume displacement) to its bulk density. Qualitative observations also suggested that lower drying intensities (i.e., reduced temperature and/or gas velocity) resulted in denser, less porous particles. Figure 2(B) illustrates the significant shrinkage that was observed throughout all trials, with the smallest particle size resulting from the mildest drying intensity of 88 °C.

From Table 3, rapid/intensive heating resulted in reduced shrinkage. Additional qualitative assessment also found the particles to be more porous. An increase in

particle size appeared to correlate with a reduction in relative shrinkage, although this may be attributed to larger particles experiencing less intensive heating than smaller ones under the same set of conditions. Fraikin et al.[30] observed a similar phenomenon, where intensive drying processes (high gas velocity and high temperature) produced particles with larger volume and higher porosity compared to milder conditions. Intensive drying/rapid evaporation does not allow the biosolids sufficient time to readjust their structure before the crust 'sets'. Conversely, slow drying flux enables the sludge structure to adjust, resulting in smaller and more compact particles.

By controlling drying conditions, biosolids producers can fine tune their product to suit specific applications. For example, applications like landscaping or agriculture might favor a denser product, that concentrates minerals, whereas biosolids for more novel applications, such as an ad/absorbents, may benefit from the larger surface area offered by porous particles.

3.2. Analysis of temperature and moisture profiles during convective drying

Figure 3 shows typical MR and center temperature (T_{centre}) profiles that were consistent across all trials. The MR curves exhibit a nearly negative exponential shape, characteristic of a decreasing drying rate, also

Table 3. Particle diameter shrinkage: pre and post drying measurements with average shrinkage percentage (e.g., MSJ-138-2 cm-2.4 refers to biosolids from Mount St John, drying gas temperature of 138 °C, 2 cm initial diameter, and drying gas velocity of 2.4 m s^{-1}).

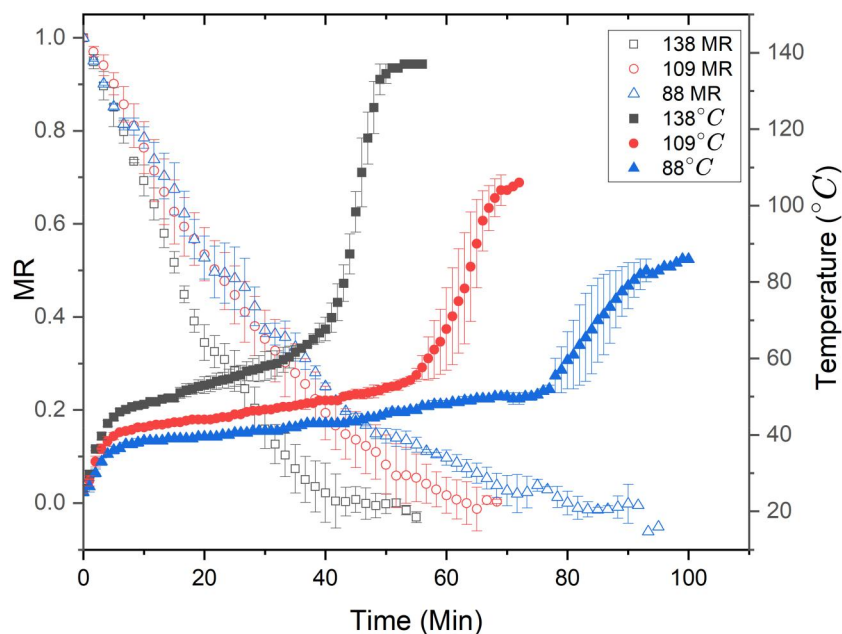| Run	Initial diameter [cm]	Final Diameter [cm]	Average Shrinkage [%]	Standard Deviation [± cm]
MSJ-138-2cm-2.4	2	1.42	29.2	0.045
MSJ-109-2cm-2.4	2	1.36	32.1	0.010
MSJ-88-2cm-2.4	2	1.34	33.2	0.024
MSJ-138-2cm-1.6	2	1.36	31.8	0.035
MSJ-138-4cm-1.6	4	2.85	28.8	0.062
MSJ-138-4cm-2.4	4	3.31	17.4	0.010
CB-138-2cm-2.4	2	1.64	18.0	0.012
CB-109-2cm-2.4	2	1.49	25.4	0.023
CB-88-2cm-2.4	2	1.44	28.0	0.035
CB-138-4cm-2.4	4	3.62	17.8	0.027

Figure 3. Impact of drying gas temperature on internal temperature and MR profiles. Legend indicates drying gas temperature. Particle size was 2 cm and gas velocity was 2.4 ms^{-1}

known as a falling rate period. The T_{centre} profiles demonstrate an initial rapid rise to the drying gas wet-bulb temperature, followed by a quasi-constant phase of gradual temperature increase, and then a sharp rise to reach thermal equilibrium with the drying gas temperature. The final rise is presumed to correspond to rapid heating after all moisture had evaporated. In contrast, the surface temperature measurements (Figure 4) were significantly higher, showing a more linear rise to T_{gas}. These measurements coupled with the center temperature measurements, indicate a notable temperature gradient throughout the particle. Additionally, IR images revealed subsurface temperatures were notably lower than surface temperatures, as highlighted in Figure 5. These subsurface temperatures represent the intermediate area between the core and surface, rather than the core itself. Significant temperature differences between surface and subsurface areas have also been observed by Novak et al.[24] and Lipolt et al.[25] Novak et al.

expanded on the work of Lipolt et al. by convectively drying 4–6 kg of biosolids in layers of 0.5 m × 0.5 m × 40 mm (W × D × H) on a grate, using relatively low temperatures and air velocities ranging from 65 °C to 80 °C and 0.44 to 0.78 m/s. Their infrared images clearly showed a large temperature variation between the surface and subsurface regions of the biosolids.

Changes in gas velocity, gas temperature, and particle size did not affect these overarching trends, but did influence the total duration of drying processes. Both mass/MR curves and temperature profiles found in this study are similar to what other researchers have found.[24,25,27,30,38]

The rate of temperature during the quasi-constant temperature increase appeared dependent on the drying gas temperature, with hotter drying gas temperatures producing a more pronounced rise in temperature away from the wet bulb temperature. Additionally, hotter drying gas temperatures
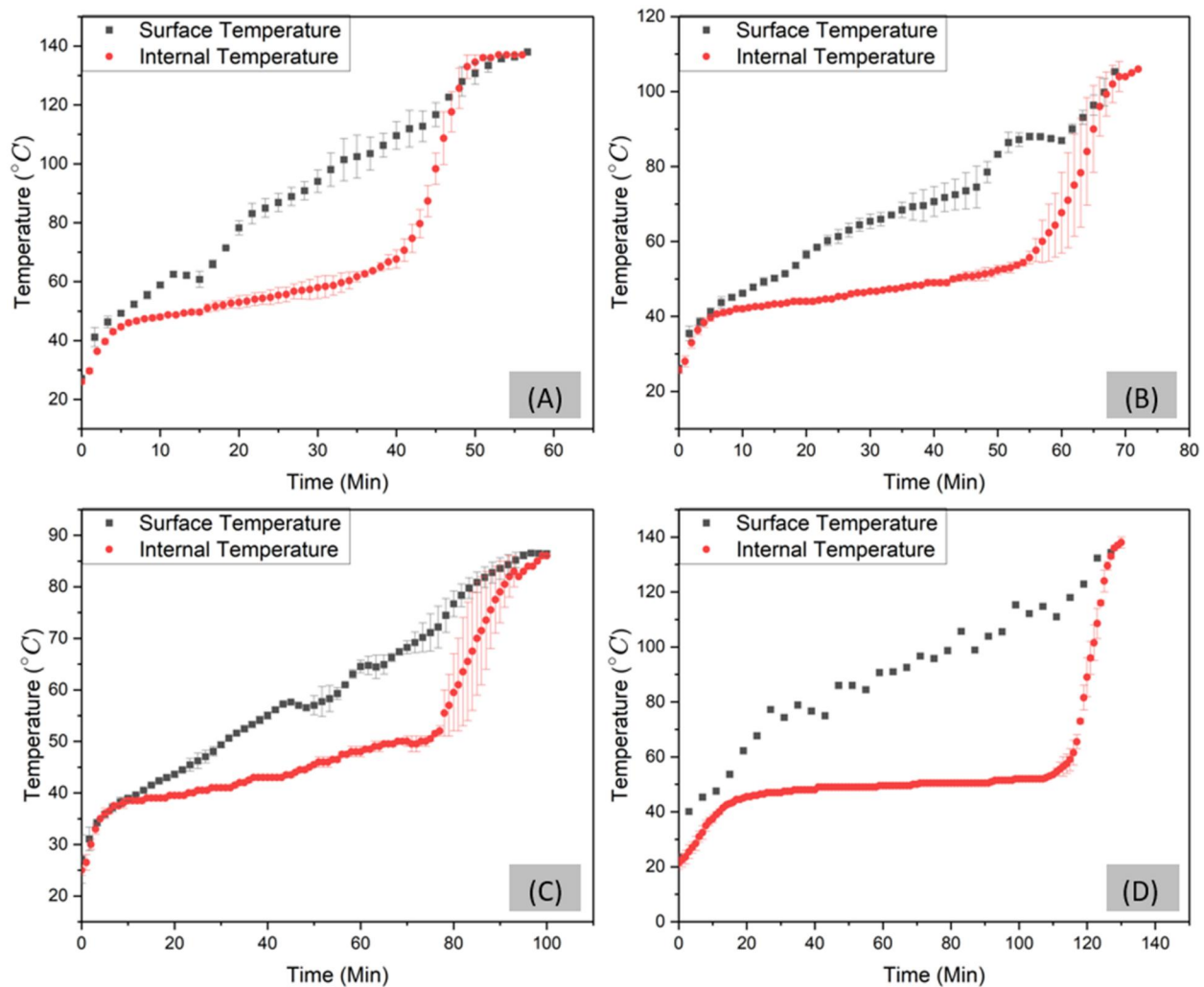
Figure 4. Comparison of internal and surface temperatures for various conditions. All graphs have a drying gas velocity of 2.4 m/s. (A–C) are 2 cm particles with drying gas temperatures of 138 °C, 109 °C, and 88 °C, respectively. (D) is a 4 cm particle with a drying gas temperature of 138 °C.

resulted in a faster/higher 'spike' rate during the final period of drying. This behavior has been observed in other studies, such as Font et al.[27] However, Font et al. attributed this phenomenon to moisture evaporation occurring at the thermocouple rather than significant internal temperature gradients. The higher surface temperature and the core temperature being near the wet bulb strongly suggest the presence of a drying front. The cooler internal temperature was likely maintained due to evaporative cooling at the drying front location, where the evaporation of moisture absorbs heat, keeping the core temperature lower. Furthermore, visible images of an incompletely dried particle clearly delineated a homogeneous wet core and a porous skin/crust layer, further implying the existence of a drying front which moves radially inwards as the particle heats and dries.

3.3. Influence of particle size and drying gas temperature on drying rate profiles

Figure 6(A) illustrates the drying rate trends $\left(\frac{dMR}{dt}\right)$ observed in the majority of the trials. The drying rates initially exhibit a phase of nearly constant drying rate until approximately 0.5–0.4 MR, where they then transition to a falling rate period. In contrast, Figure 6(B) shows an exception to this trend, represented by the 2 cm CB samples, which only displayed a falling rate period. All other samples showed both a constant rate followed by a falling rate period. Both figures clearly indicate that increased drying gas temperature results in higher drying rates. However, when particle size was increased to 4 cm (Figure 7), both MSJ and CB samples exhibited the same behavior of a constant rate period followed by a falling rate period. The presence of a constant rate drying period typically indicates that drying is controlled by external factors, such as convective heat and mass transfer at the

material's surface, signifying sufficient moisture levels to maintain surface saturation. Conversely, the falling rate period suggests that internal factors such as diffusion (where moisture must permeate through the particle) or the development of a shrinking core (where reduced surface area, increased resistance to mass transfer due to crust formation, and increased diffusion pathways), begin to limit the rate of moisture removal.

Comparison of results to literature is difficult due to different biosolids potentially showing different drying behavior depending on their origin, as observed in this study. For example, Tao and Lee[39] and Font et al.[27] found biosolids to only display a falling rate with an absence of a constant rate when drying in a convective system.[27,39] Conversely, Leonard et al.[29] found differing behavior between their two sludge samples, with one sample displaying a constant drying rate period mainly controlled by external/convective limitations, whereas the other showed no constant drying period and was characterized by internal diffusion limitations. Similarly, Bennamoun[38] noted significant differences when drying a single particle (2.5 g, 15 mm cylinder) compared to a bed of particles (250 g, 10 mm diameter

extrudates). The single particle exhibited only a falling rate, while the particle bed experienced both a constant and falling rate period.

Figure 8 illustrates the effect of particle size on the MR and internal temperature profiles for both MSJ and CB samples, comparing 2 cm and 4 cm particles. Figure 7 demonstrates the impact of particle size on the drying rate for these same particles.

Based on Figures 7 and 8, it is evident that particle size significantly influences both the drying rate and drying time. An increase in particle size diameter by a factor of 2 (resulting in an 8-fold increase in particle volume) led to an order of magnitude reduction in drying rate, and hence an increased drying time. This substantial decrease in drying rate can be attributed to several factors: (1) Reduced surface area to volume ratio. Larger particles have a smaller surface area relative to their volume, resulting in a reduced contact area available for moisture transfer with the surrounding medium. Hence, there is a reduction in heat and mass transfer. (2) Particle mass: Larger particles have more mass, requiring more heat to raise the temperature and initiate the drying process. (3) Diffusion Path length: The distance moisture travels, whether it is liquid moisture diffusion or vapor escaping from the pores inside the particle, is increased in larger particles. Additionally, the pore structure of large particles may be less well-connected or have narrower channels, increasing the difficulty for moisture to escape.

Temperature profiles for the 4 cm particles are consistent with the 2 cm ones, however the core/internal temperatures of the large particles are more stable (i.e., the internal temperatures of the 2 cm particles experience a more pronounced upwards drift).

Statistical analysis was performed to evaluate the impact of biosolids origin on total drying times. ANOVA tests

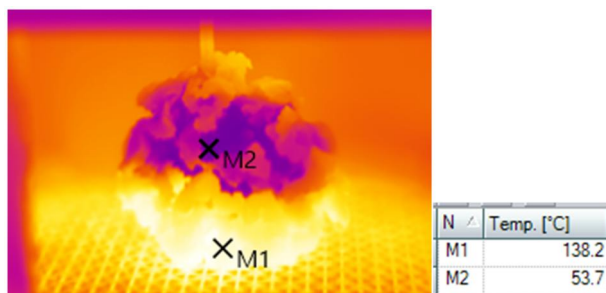| N	Temp. [°C]
M1	138.2
M2	53.7

Figure 5. IR image of biosolids particle showing significantly cooler sub-surface temperatures.
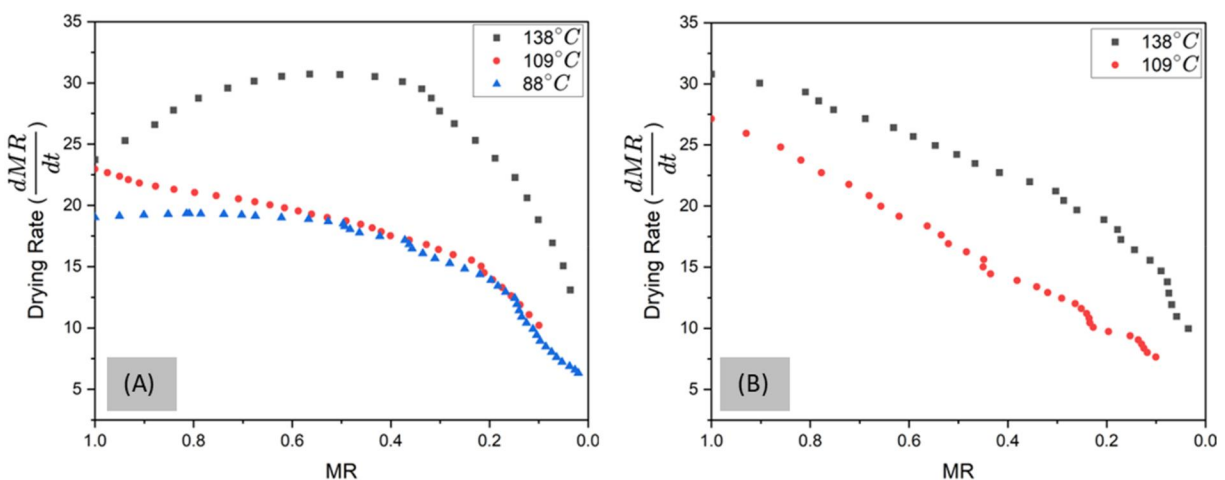

Figure 6. Representative drying rate curves. Both (A) and (B) have a drying gas velocity of 2.4 ms^{-1} and particle diameters of 2 cm. (A) MSJ samples showing two drying periods. (B) CB samples showing only a falling rate period.
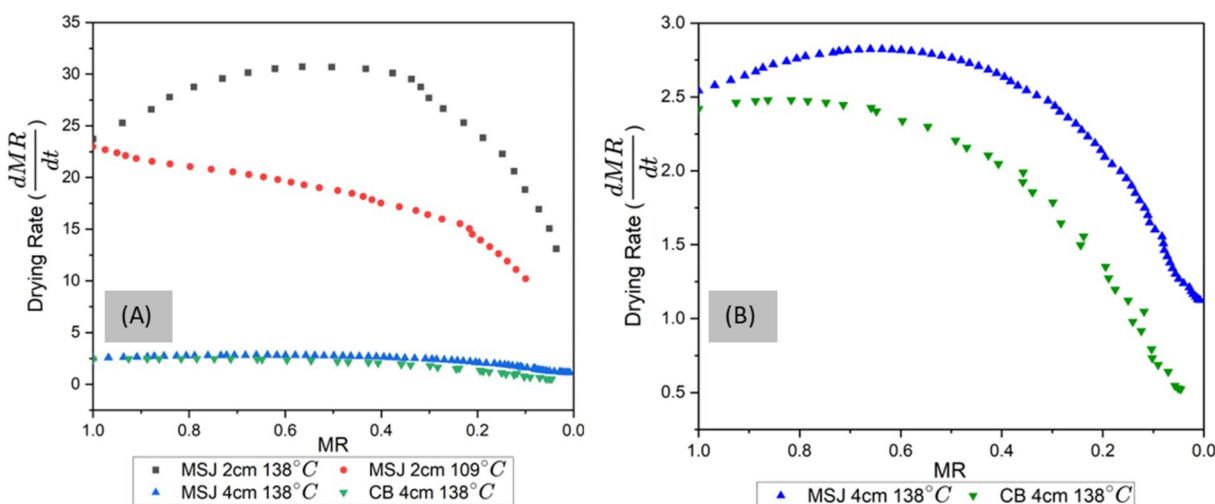
Figure 7. Impact of particle size on drying rate. Legend indicates the temperature used. All tests were conducted under 2.4 ms^{-1} drying gas velocity. (A) 2 cm and 4 cm particles; (B) 4 cm particles from MSJ and CB.
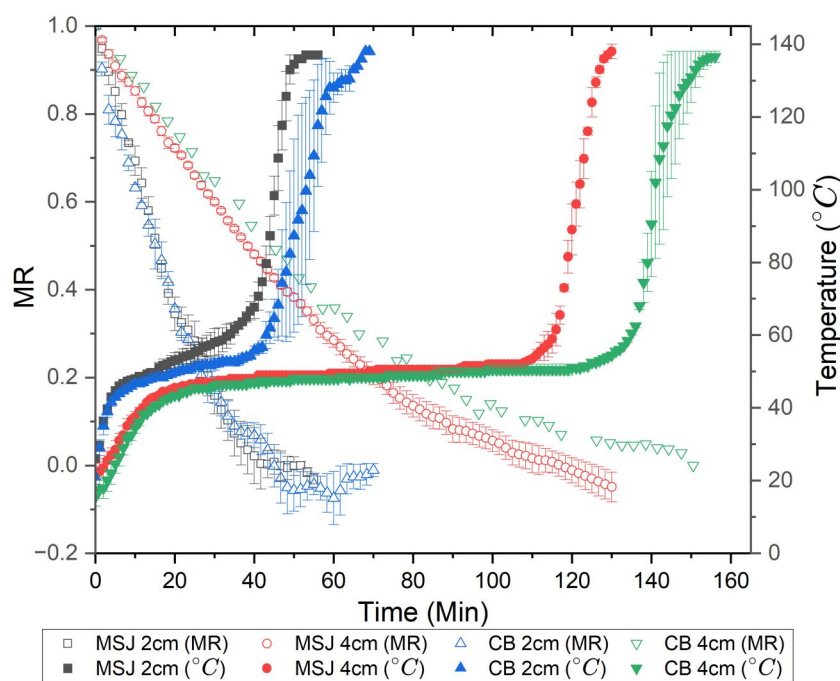

Figure 8. Impact of particle size (2 cm and 4 cm) on internal temperature and MR profiles. Drying conditions were 138 °C and 2.4 ms^{-1}.

conducted at a 0.05 significance level showed that there was no statistically significant difference between the different types of biosolids for the 2 cm particles. However, when particle size was increased to 4 cm the difference in drying time was found to be statistically significant. In the smaller particles, the ratio of the surface area to volume is higher, allowing for more efficient heat and mass transfer. This increased drying efficiency masks the underlying differences in material properties, such as thermal conductivity, diffusivity, and porosity. However, when particle size is increased to 4 cm, this efficiency decreases, and intrinsic material properties play a more significant role.

3.4. Influence of gas temperature and velocity on biosolids drying

From all measured parameters (MR vs time, central temperature vs time, drying rate vs time) it is evident that increased drying gas temperature decreased total drying time and increased the drying rate. To determine the shape of this correlation, the completed drying time was plotted against gas temperature, as shown in Supplementary Figure S2.

ANOVA testing (significance level 0.05) showed that drying gas temperature had a statistically significant impact on drying time. However, increasing temperature
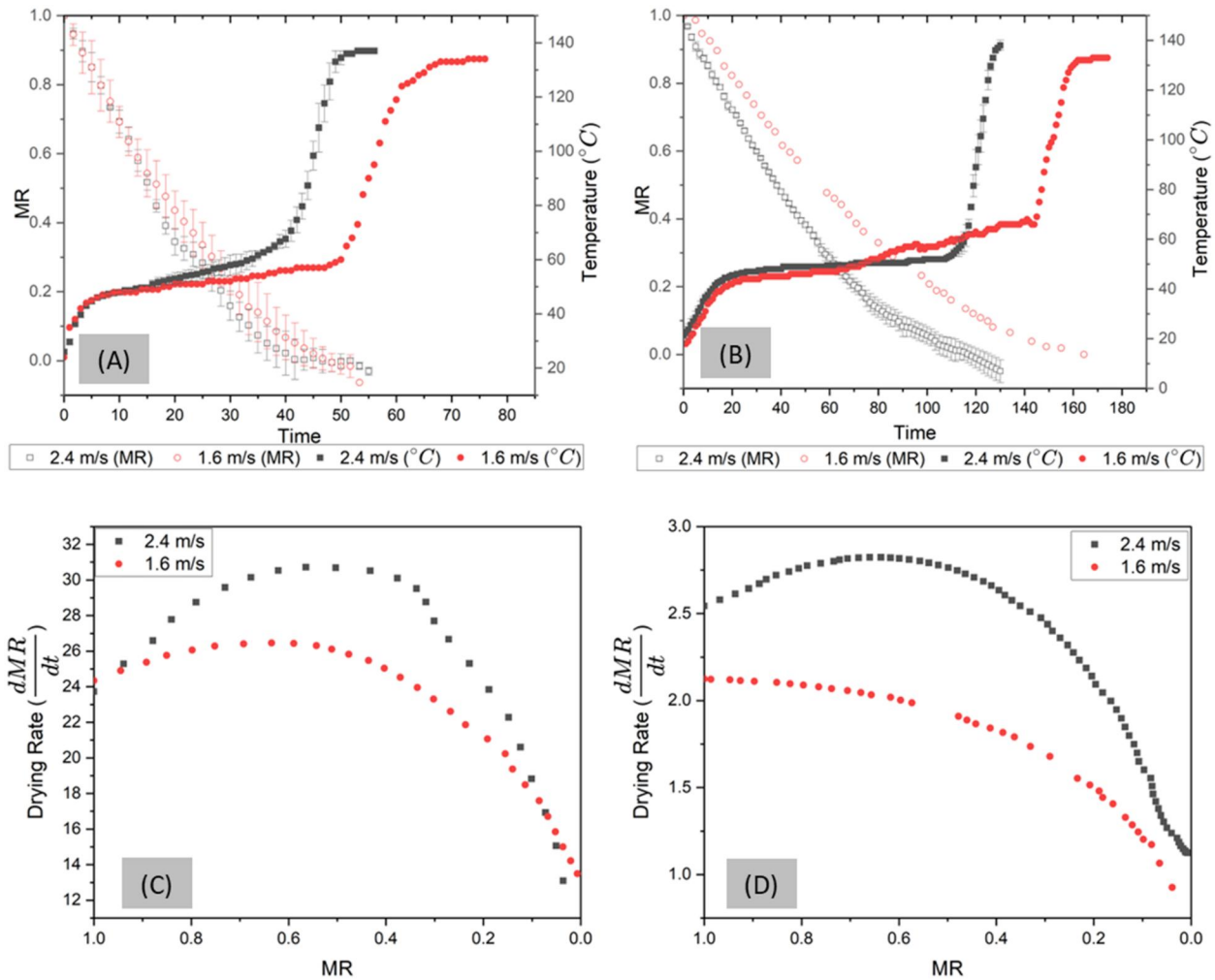
Figure 9. Impact of gas velocity on internal temperature, MR profiles, and drying rates for MSJ biosolids. Temperature for all graphs was 138 °C. (A) 2 cm particles; (B) 4 cm particles; (C) Drying rates for 2 cm particles; (D) Drying rates for 4 cm particles.

did not result in a directly proportional decrease in drying time, with a potential plateau effect beyond 109 °C, as shown in Supplementary Figure S2. This finding partially agrees with the study by Zhao et al,[40] which focused on radiative drying rather than convective, and found no significant gains in drying rate above 120 °C. This potential plateau indicates that at higher drying temperatures, diffusion limitations may be rate-limiting, whereas at lower drying gas temperatures, heat transfer may be the rate limiting step.

Figure 9 highlights the impact of gas velocity on MR and internal temperature profiles, and drying rates, respectively. Experiments were performed at a temperature of 138 °C, with gas velocities of 2.4 m/s and 1.6 m/s, respectively. The drying rates shown in Figure 9(C,D) were found to be a function of gas velocity, with the impact being more pronounced as particle size increased. This is consistent with the assumption that the drying rate is initially heat transfer limited rather than the system being diffusion limited. In heat

transfer limited systems, the surrounding air's capacity to absorb moisture serves as the limiting factor, resulting in an inability to maintain a low humidity level necessary for a high rate of evaporation. This finding contrasts Bellur et al,[41] which found that in a fluidized bed dryer, the drying of biosolids was independent of gas velocity and was solely a function of temperature, indicating primarily diffusion limited drying. Therefore, the limiting factors may be specific to the biosolids being dried, emphasizing the importance of tailoring drying systems and conditions to the specific characteristics/properties of the biosolids being dried.

4. Conclusion

Internal temperature measurements, regardless of biosolids origin, gas temperatures, or particle diameters, showed a consistent pattern: an initial heating period, a prolonged quasi-constant temperature roughly at the

drying gas's wet bulb temperature, followed by a sharp increase to T_{gas} in the final moments of drying. In contrast, the surface temperature measurements were significantly higher, indicating a notable temperature gradient throughout the particle. These temperature profiles support the involvement of multiple drying mechanisms.

The linearity of the surface temperature suggests that the primary mechanism is external heat transfer from the surrounding environment. The extended period of quasi-constant central temperature suggests that moisture removal is balanced with the rate of heat transfer from the surface, characteristic of constant rate drying. Furthermore, the quasi-constant core temperature during the falling rate phase implies a balance between heat transfer to the core and the evaporative cooling effect from moisture removal.

This testing also highlights the importance of managing particles size in thermal processing, emphasizing the use of the smallest feasible biosolids particle size to reduce drying times and enhance drying efficiency. Additionally, the tests have demonstrated that the central temperature remains near the wet bulb temperature across most of the drying process, which could significantly impact the system's ability to remove or destroy contaminants.

Declaration of Interest Statement

The authors report no conflicts of interest. The authors alone are responsible for the content and writing of the paper.

ORCID

Julian Nylen (iD) http://orcid.org/0000-0003-0965-4564
Elsa Antunes (iD) http://orcid.org/0000-0003-4246-7824

References

[1] Torri, S. I.; Corrêa, R. S.; Renella, G. Soil Carbon Sequestration Resulting from Biosolids Application. *Appl. Environ. Soil Sci.* **2014**, *2014*, 1–9. DOI: 10.1155/2014/821768.

[2] Sharma, B.; Sarkar, A.; Singh, P.; Singh, R. P. Agricultural Utilization of Biosolids: A Review on Potential Effects on Soil and Plant Grown. *Waste Manag.* **2017**, *64*, 117–132. DOI: 10.1016/j.wasman.2017.03.002.

[3] Clarke, B. O.; Smith, S. R. Review of 'Emerging' Organic Contaminants in Biosolids and Assessment of International Research Priorities for the Agricultural Use of Biosolids. *Environ. Int.* **2011**, *37*, 226–247. DOI: 10.1016/j.envint.2010.06.004.

[4] Marchuk, S.; Tait, S.; Sinha, P.; Harris, P.; Antille, D. L.; McCabe, B. K. Biosolids-Derived Fertilisers: A Review of Challenges and Opportunities. *Sci. Total Environ.* **2023**, *875*, 162555. DOI: 10.1016/j.scitotenv.2023.162555.

[5] Moodie, D.; Coggan, T.; Berry, K.; Kolobaric, A.; Fernandes, M.; Lee, E.; Reichman, S.; Nugegoda, D.; Clarke, B. O. Legacy and Emerging per- and Polyfluoroalkyl Substances (PFASs) in Australian Biosolids. *Chemosphere* **2021**, *270*, 129143. DOI: 10.1016/j.chemosphere.2020.129143.

[6] Kuskopf, L.; Sheehan, M.; Whelan, A. Contaminants of Emerging Concern: Developing a Sampling and Analysis Quality Plan for the Cleveland Bay Sewage Treatment Plant. *Water J.* **2020**, *5*, 1–28. https://web.archive.org/web/20201214000856id_/https://water-source.awa.asn.au/wp-content/uploads/2020/12/WEJ_2020_019.pdf. DOI: 10.21139/wej.2020.019.

[7] Rahman, S. M.; Eckelman, M. J.; Onnis-Hayden, A.; Gu, A. Z. Comparative Life Cycle Assessment of Advanced Wastewater Treatment Processes for Removal of Chemicals of Emerging Concern. *Environ. Sci. Technol.* **2018**, *52*, 11346–11358. DOI: 10.1021/acs.est.8b00036.

[8] Tran, N. H.; Reinhard, M.; Gin, K. Y.-H. Occurrence and Fate of Emerging Contaminants in Municipal Wastewater Treatment Plants from Different Geographical Regions-a Review. *Water Res.* **2018**, *133*, 182–207. DOI: 10.1016/j.watres.2017.12.029.

[9] Golovko, O.; Örn, S.; Sörengård, M.; Frieberg, K.; Nassazzi, W.; Lai, F. Y.; Ahrens, L. Occurrence and Removal of Chemicals of Emerging Concern in Wastewater Treatment Plants and Their Impact on Receiving Water Systems. *Sci. Total Environ.* **2021**, *754*, 142122. DOI: 10.1016/j.scitotenv.2020.142122.

[10] Joo, S.; Dello Monaco, F.; Antmann, E.; Chorath, P. Sustainable Approaches for Minimizing Biosolids Production and Maximizing Reuse Options in Sludge Management: A Review. *J. Environ. Manage.* **2015**, *158*, 133–145. DOI: 10.1016/j.jenvman.2015.05.014.

[11] Coggan, T. L.; Moodie, D.; Kolobaric, A.; Szabo, D.; Shimeta, J.; Crosbie, N. D.; Lee, E.; Fernandes, M.; Clarke, B. O. An Investigation into per- and Polyfluoroalkyl Substances (PFAS) in Nineteen Australian Wastewater Treatment Plants (WWTPs). *Heliyon* **2019**, *5*, e02316. DOI: 10.1016/j.heliyon.2019.e02316.

[12] Wang, W.; Rhodes, G.; Ge, J.; Yu, X.; Li, H. Uptake and Accumulation of per- and Polyfluoroalkyl Substances in Plants. *Chemosphere* **2020**, *261*, 127584. DOI: 10.1016/j.chemosphere.2020.127584.

[13] Dodgen, L. K.; Li, J.; Parker, D.; Gan, J. J. Uptake and Accumulation of Four PPCP/EDCs in Two Leafy Vegetables. *Environ. Pollut.* **2013**, *182*, 150–156. DOI: 10.1016/j.envpol.2013.06.038.

[14] Mohajerani, A.; Karabatak, B. Microplastics and Pollutants in Biosolids Have Contaminated Agricultural Soils: An Analytical Study and a Proposal to Cease the Use of Biosolids in Farmlands and Utilise Them in Sustainable Bricks. *Waste Manag.* **2020**, *107*, 252–265. DOI: 10.1016/j.wasman.2020.04.021.

[15] Ghisi, R.; Vamerali, T.; Manzetti, S. Accumulation of Perfluorinated Alkyl Substances (PFAS) in Agricultural Plants: A Review. *Environ. Res.* **2019**, *169*, 326–341. DOI: 10.1016/j.envres.2018.10.023.

[16] Sinha, P.; Marchuk, S.; Harris, P.; Antille, D. L.; McCabe, B. K. Land Application of Biosolids-Derived Biochar in Australia: A Review. *Sustainability* **2023**, *15*, 10909. https://www.mdpi.com/2071-1050/15/14/10909. DOI: 10.3390/su151410909.

[17] Patel, S.; Kundu, S.; Halder, P.; Ratnnayake, N.; Marzbali, M. H.; Aktar, S.; Selezneva, E.; Paz-Ferreiro, J.; Surapaneni, A.; de Figueiredo, C. C.; et al. A Critical Literature Review on Biosolids to Biochar: An Alternative Biosolids Management Option. *Rev. Environ. Sci. Biotechnol.* **2020**, *19*, 807–841. DOI: 10.1007/s11157-020-09553-x.

[18] Gao, N.; Kamran, K.; Quan, C.; Williams, P. T. Thermochemical Conversion of Sewage Sludge: A Critical Review. *Prog. Energy Combust. Sci.* **2020**, *79*, 100843. DOI: 10.1016/j.pecs.2020.100843.

[19] Chen, G.; Lock Yue, P.; Mujumdar, A. S. Sludge Dewatering and Drying. *Dry. Technol.* **2002**, *20*, 883–916. DOI: 10.1081/DRT-120003768.

[20] McNamara, P. J.; Koch, J. D.; Liu, Z.; Zitomer, D. H. Pyrolysis of Dried Wastewater Biosolids Can Be Energy Positive. *Water Environ. Res.* **2016**, *88*, 804–810. DOI: 10.2175/106143016x14609975747441.

[21] Winchell, L. J.; Ross, J. J.; Wells, M. J. M.; Fonoll, X.; Norton, J. W.; Bell, K. Y. Per- and Polyfluoroalkyl Substances Thermal Destruction at Water Resource Recovery Facilities: A State of the Science Review. *Water Environ. Res.* **2021**, *93*, 826–843. DOI: 10.1002/wer.1483.

[22] Deng, R.; Wang, L.; Zhang, R.; Luo, Y. Pyrolysis Behaviors of Thermally-Thick Sewage Sludge Particle with High Moisture Content: An Experimental and Modelling Study. *Fuel* **2021**, *305*, 121442. DOI: 10.1016/j.fuel.2021.121442.

[23] Altarawneh, M. A Chemical Kinetic Model for the Decomposition of Perfluorinated Sulfonic Acids. *Chemosphere* **2021**, *263*, 128256. DOI: 10.1016/j.chemosphere.2020.128256.

[24] Novak, L.; Širok, B.; Zupanc, M.; Hočevar, M. Effects of Layer Inhomogeneities on the Process of Sewage Sludge Convective Drying. *Drying Technol.* **2024**, *42*, 34–47. DOI: 10.1080/07373937.2023.2259974.

[25] Lipolt, A.; Širok, B.; Hočevar, M.; Novak, L. Convective Drying of Sewage Sludge Layer in Through-Flow. *J. Mech. Eng.* **2020**, *66*, 13. DOI: 10.5545/sv-jme.2020.6717.

[26] Reyes, A.; Eckholt, M.; Troncoso, F.; Efremov, G. Drying Kinetics of Sludge from a Wastewater Treatment Plant. *Dry. Technol.* **2004**, *22*, 2135–2150. DOI: 10.1081/DRT-200034218.

[27] Font, R.; Gomez-Rico, M. F.; Fullana, A. Skin Effect in the Heat and Mass Transfer Model for Sewage Sludge Drying. *Sep. Purif. Technol.* **2011**, *77*, 146–161. DOI: 10.1016/j.seppur.2010.12.001.

[28] Bennamoun, L.; Arlabosse, P.; Léonard, A. Review on Fundamental Aspect of Application of Drying Process to Wastewater Sludge. *Renew. Sustain. Energy Rev.* **2013**, *28*, 29–43. DOI: 10.1016/j.rser.2013.07.043.

[29] Léonard, A.; Blacher, S.; Marchot, P.; Pirard, J. P.; Crine, M. Convective Drying of Wastewater Sludges: Influence of Air Temperature, Superficial Velocity, and Humidity on the Kinetics. *Dry. Technol.* **2005**, *23*, 1667–1679. DOI: 10.1081/DRT-200065082.

[30] Fraikin, L.; Herbreteau, B.; Salmon, T.; Nicol, F.; Crine, M.; Léonard, A. Use of an Experimental Design to Characterize the Convective Drying Behavior of Different Sludges. *Dry. Technol.* **2015**, *33*, 1302–1308. DOI: 10.1080/07373937.2015.1026979.

[31] Bezzina, G.; Sheehan, M.; Walker, C. The Influence of Gas Velocity and Fibre Density on the Drying Kinetics of Bagasse. *Proceedings of the 40th Annual Conference of the Australian Society of Sugar Cane Technologists*, **2018**, 424–435. https://researchonline.jcu.edu.au/58507/.

[32] Walker, C.; Sheehan, M. Drying Kinetics of Macroalgae as a Function of Drying Gas Velocity and Material Bulk Density, Including Shrinkage. *Clean Technol.* **2022**, *4*, 669–689. DOI: 10.3390/cleantechnol4030041.

[33] Mäkelä, M.; Edler, J.; Geladi, P. Low-Temperature Drying of Industrial Biosludge with Simulated Secondary Heat. *Appl. Therm. Eng.* **2017**, *116*, 792–798. DOI: 10.1016/j.applthermaleng.2017.02.010.

[34] Hippinen, I.; Ahtila, P. Drying of Activated Sludge Under Partial Vacuum Conditions—An Experimental Study. *Dry. Technol.* **2004**, *22*, 2119–2134. DOI: 10.1081/DRT-200034247.

[35] Nylen, J.; Sheehan, M. Review of the Integration of Drying and Thermal Treatment Processes for Energy Efficient Reduction of Contaminants and Beneficial Reuse of Wastewater Treatment Plant Biosolids. *Energies* **2023**, *16*, 1964. https://www.mdpi.com/1996-1073/16/4/1964. DOI: 10.3390/en16041964.

[36] Logan City Council. Technical Report Loganholme Waste-Water Treatment Plant: Biosolids Gasification Demonstration Project. (PBE-075). **2021**. https://arena.gov.au/assets/2021/03/loganholme-wastewater-treatment-plant.pdf.

[37] Bennamoun, L.; Crine, M.; Léonard, A. Convective Drying of Wastewater Sludge: Introduction of Shrinkage Effect in Mathematical Modeling. *Dry. Technol.* **2013**, *31*, 643–654. DOI: 10.1080/07373937.2012.752743.

[38] Bennamoun, L.; Fraikin, L.; Li, J.; Léonard, A. Forced Convective Drying of Wastewater Sludge with the Presentation of Exergy Analysis of the Dryer. *Chem. Eng. Commun.* **2016**, *203*, 855–860. DOI: 10.1080/00986445.2015.1114475.

[39] Tao, T.; Peng, X. F.; Lee, D. J. Structure of Crack in Thermally Dried Sludge Cake. *Dry. Technol.* **2005**, *23*, 1555–1568. DOI: 10.1081/DRT-200063547.

[40] Zhao, G.; Yin, F.; Liang, X.; Yuan, D.; Geng, W.; Wang, L.; Sun, R. Drying Experiment and Drying Model Analysis of Dehydrated Sludge Particles. *IOP Conf. Ser: Mater. Sci. Eng.* **2020**, *768*, 022031. DOI: 10.1088/1757-899X/768/2/022031.

[41] Bellur, S. R.; Coronella, C. J.; Vásquez, V. R. Analysis of Biosolids Equilibrium Moisture and Drying. *Env. Prog. Sustain. Energy* **2009**, *28*, 291–298. DOI: 10.1002/ep.10353.